

ACTIVE FLOW CONTROL FOR TURBULENT SEPARATED FLOWS

D. Skamnakis and K.Papailiou

Phd Student and Professor
Laboratory of Thermal Turbomachines
National Technical University of Athens
Athens, GREECE

ABSTRACT

Linear Orr – Somerfeld type stability analysis is proposed as a tool to indicate the position and the pulsation frequency of a pulsating slot. Analysis is extended to turbulent flows using URANS equations. The concept is tested to a ducted case and applied to a linear compressor cascade. Additionally a numerical study is conducted to analyze compressor surge margin gain through steady blowing injection, sensed as rotating by the rotor.

INTRODUCTION

During the last years, active flow control techniques addressing the unsteady nature of the flow have gained interest (see Greenblatt and Wygnansky 2000). Hydrodynamic periodic excitation is used to decrease, in the mean, existing separation regions (indicatively Seifer et al, Bons et al, Volino 2003, Xinqian et al 2004). In this paper it is proposed to make use of stability analysis as guide for effective active flow control using synthetic (or pulsating) jets. This concept is applied to a 2D experimental case for verification (see also Skamnakis and Papailiou 2005), and subsequently to a 2D compressor linear cascade with flow separation present (see also Skamnakis and Papailiou 2006).

Periodic excitation is finally used in order to investigate surge margin displacement of a 3D compressor rotor, applying distinct continuous blowing at the inlet. Preliminary results are reported for this case, which complements the previously described computational approach, for applying flow control on compressors.

STABILITY ANALYSIS FOR FLOW CONTROL

For an effective and affordable active flow control, a minimum of kinetic energy should be provided externally. In order to comply with this demand, the small vortical structures which are generated through synthetic or pulsating jets, must grow and transfer momentum to the separated flow region in need. The vortical structure frequency (equal to that of the pulsating jets) becomes a key factor and stability analysis is necessary in order to establish the most unstable modes for vortical structure amplification.

In order to validate this statement a 2D flow is considered with a train of elementary spanwise vortices, introduced as a perturbation from the solid wall. In the actual case these can be generated experimentally using a slot with a pulsating injection device. For optimizing this situation, two main parameters will have to be considered, in the first case: the position of the slot and the pulsation frequency. To define completely the slot geometry and its pulsation characteristics, its blowing direction and pulsation amplitude will also have to be specified. The choices of the first two parameters mentioned above are made through stability analysis results. The last two will be considered later.

Stability analysis is already developed for laminar flows in relation to transition from laminar to turbulent flow. The same equation may be used to handle flow control problems for laminar flow, because the computed modes are valid for both velocity and vorticity fluctuations. In order to obtain an extension to turbulent flows, exactly the same procedure may be followed (see Schlichting 2000), using instead of the UNS, the URANS equations. In this last case and for the present work, the Bousinesque hypothesis is used for closure.

In using an eddy viscosity hypothesis, stability analysis and simulation is valid for frequencies, which are far from those characterizing the phenomenon of turbulence. This is not particularly restrictive to the present case, because the regular structures generated and used very often for flow control, are larger in magnitude and characterized by lower time scales than those of turbulence. That is confirmed experimentally, where optimal frequencies are applied, resulting to a Strouhal number close to unity (indicatively Seifert et al. 1999b, Greenblat and Wygnanski 2000). In that sense the fact of using eddy viscosity is not restrictive.

Consequently using the URANS equations and performing the same procedure, the following extended (Orr-Sommerfeld like) equation is obtained (see Skamnakis and Papailiou 2006):

$$\psi(x, y, t) \rightarrow \phi(y)e^{ax+ibt}, \quad a \in \mathbb{C}, \quad b \in \mathbb{R}$$

$$(U - i\frac{b}{a})(\phi'' - a^2\phi) - U''\phi = -i\frac{v'_{eff}}{a}(\phi'''' - 2a^2\phi'' + a^4\phi) - i\frac{1}{a}(a^2\phi + \phi'')v''_{eff} - i\frac{1}{a}(-a^2\phi' + \phi''')v'_{eff}$$

additional terms due to turbulence

where $U(y)$ is a velocity profile and $\psi(x,y,t)$ is a stream function for the velocity perturbations. The same equation is obtained when considering transition with heated or cooled walls. Then viscosity varies with temperature and its derivatives appear in the formulation. However, to our knowledge, it is the first time this equation is used with the eddy viscosity assumption for turbulent flows.

The above equation describes an eigenvalue problem, for each defined wavelength $Re[\alpha]$, where b and $\phi(y)$ are defined. Each mode $\phi(y)e^{ax+ibt}$ is equivalent with a train of vortices of diameter (along x) of π/α , traveling with velocity $-\text{Im}[b]/\alpha$ and with a growing rate of $e^{\text{Re}[b]t}$ in time. Such a mode should be generate by a jet operating at a frequency of $f=(\text{traveling velocity})/(\text{wave length})$ that equals to $\text{Im}[b]/2\pi$. Consequently selecting among the modes the most unstable the pulsation frequency is defined.

The above analysis is performed on a boundary layer profile, using a parallel flow approximation and has a local character. This analysis can be used to find the most advantageous position of the controlling jet. It is performed for several positions along the solid surface. The choice of the optimal mode is made, taking in to account simultaneously all positions from where each generated vorticity perturbation will pass. The jet is placed usually just upstream of the region where it starts to be unstable. The corresponding procedure is discussed in the following two sections.

COMPARING WITH EXPERIMENTAL RESULTS

In order to describe and test the concept introduced above, a stability analysis is performed for a pulsating jet case, which has been investigated experimentally (see Seifert et al

1999a,1999b,2000). Performing a stability analysis for each position for several wavelengths and extracting, each time, the most unstable discrete mode, figure 1 is constructed. For each jet position x_{jet} the exponential growth of the perturbation is given in terms of the the applied jet frequency. The generated vortex trajectory is following a constant frequency line. Optimal results can be obtained when, along the generated vortex trajectory, areas with high exponential growth are encountered, for an as large length as possible. In figure 1 optimal frequencies found experimentally (by Seifert for the specific experiment or derived from more experiments by Greenblat and Wygnanski 2000) are compared with the one suggested by the stability analysis of figure 1. They are all quite close together.

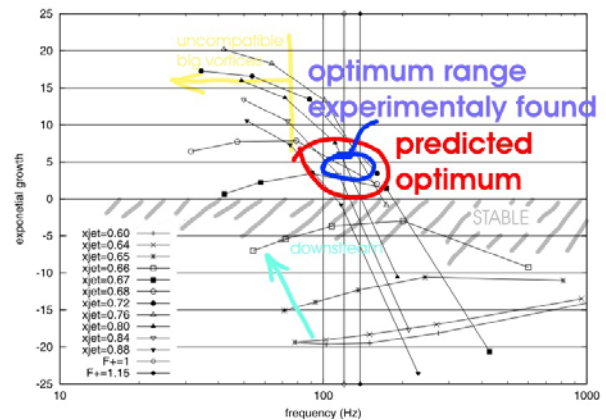


Figure 1: analysis results of growth versus frequency

This case was further simulated in similar conditions with the in-house developed CFD code and the comparison with experiment is presented in figure 2. This comparison shows satisfactory agreement for engineering applications.

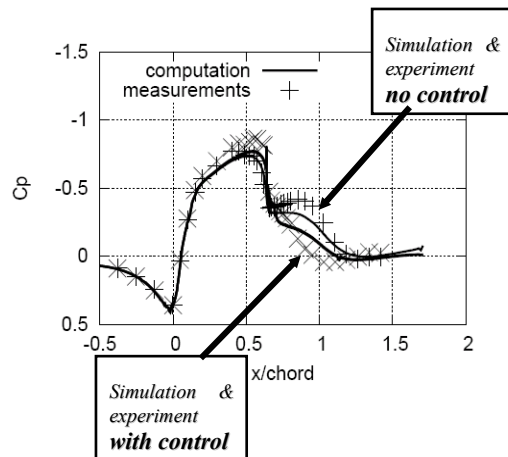


Figure 2: computation & experiment

CONTROLLING A COMPRESSOR CASCADE

In order to analyze a case closer to turbomachinery applications, a linear compressor cascade was considered (see Steiner et al, 1990) with an axial velocity density ratio $AVDR=1$ and an incidence of 5° . Under these conditions, flow is separated for a length of around 40% of the chord. In figure 3 the separated flow region is visualized using streamlines. Positions 1 to 7, where stability analysis is later performed are indicated on the same figure.

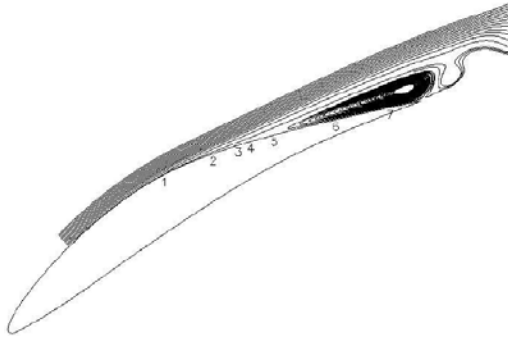


Figure 3: compressor blade & positions

Separation occurs between positions 3 and 4. The same plot of growth versus frequency, as in figure 1, is constructed and presented at figure 4. Each curve corresponds to a position of figure 3.

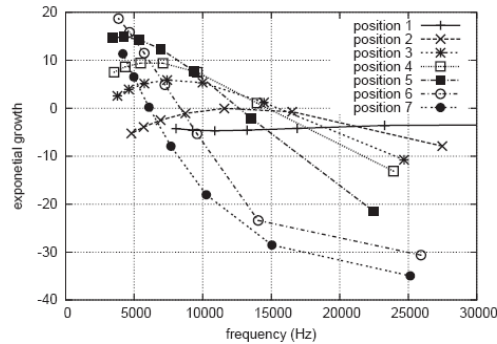


Figure 4: Growth versus frequency

Unstable modes appear starting from position 2, where almost zero growth values are present, reaching positive values in downstream positions. It is noted that growth of the vorticity perturbations increases sharply near the separation point.

An appropriate frequency, provoking high perturbation growth in most positions could be that of 7.5kHz. An appropriate position to apply that frequency is position 4, where the curve attains its maximum at that frequency. Additionally, position 4 is enough upstream, so that the perturbations will have the time and the necessary length to be generated and grow. Another choice, which is examined here, is suggested by the experiment of Zhang and Fasel 1999, which positions the jet far upstream, in an effort to maximize the vortex trajectory. The chosen position is no 2 and the chosen frequency is 12kHz.

Both choices are represented with a wavelength that is almost ten times larger than the characteristic length scale of turbulence \sqrt{k}/ω . In this way, the applied frequencies are decoupled from those of turbulence, allowing the use of URANS complemented with the Bousinesq approximation

Several simulations were performed for two position-frequency choices indicated above. The following table 1 summarizes each run.

configuration	0	1	2	3	4	5
pulsation frequency(KHz)	-	12.0	12.0	7.5	7.5	7.5
jet velocity(m/sec)	-	250	160	250	160	80
slot width/chord (%)	-	0.7	1.0	0.7	1.0	1.0
jet yaw angle ⁵ (deg)	-	45	65	45	68	68
position number	-	"2"	"2"	"4"	"4"	"4"
mean exit angle a2(deg)	26.5°	24.5°	26.0°	23.8°	24.7°	25.3°
mean losses (%)	4.0	4.2	4.5	4.7	4.6	4.5

Table 1: runs description

The flow exit angle of the cascade, used as an indication for flow control effectiveness, is plotted in figure 5.

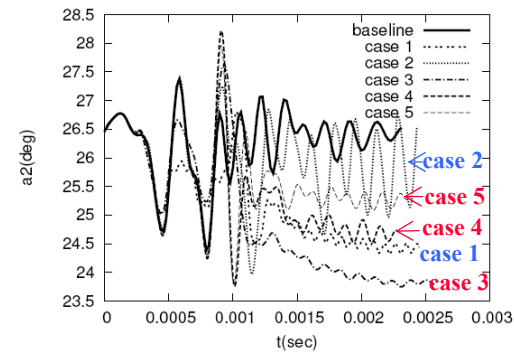


Figure 5: Computed exit angle

All runs are initiated from the same flow field, resulting from a steady state solver. The baseline run, has no slot present and is set for comparison. A settling time even for the baseline case, is necessary in order to pass from the steady to the unsteady state computation. Note that global characteristics (as for instance exit flow angle), are the same for the steady and unsteady computations of the no control case.

Angle is measured at the exit plane of the computational domain, which is 150% of the axial chord downstream of the trailing edge. This explains the hysteresis in the angle computation to reach meaningful values, of the order of one millisecond. This is the time that a particle needs to reach the exit plane.

In order to appreciate angle changes, exit angles for the air inlet angle of 47° (design value) with no separation, and the air inlet angle of 52° (case considered for the presented runs), are summarized in table 2.

	experiment		computation	
	1.1	1.1	1.0	1.0
AVDR	47.0°	52.0°	47.0°	52.0°
a1	20.4°	22.8°	23.4°	26.5°
a2	1.9	4.1	2.7	4.0
losses (%)				

Table 2: angles and losses

The differences between experiment and computation are due to the more severe, but more computationally convenient, conditions for the later case. For the calculation, the axial velocity density ratio is smaller and the shear layers are considered turbulent from the leading edge.

Considering now table 1 and figure 5, best results are obtained for case 3, (table 1), for which exit angle was decreased by more than 2.5° reaching 23.8°. This fact indicates the elimination of separation along the suction side. Comparing cases 1 and 3, which represent the two choices made for the position and frequency, (conserving the same slot width and velocity amplitude), it is remarked that flow control is effective for both. However the control for case 3 gives better results since it reduces further by 0.65° the deviation angle of case 1, and remains effective for an even lower velocity amplitude and injection angle (cases 4,5). On the other hand, changing, for case 2, the injection angle of case 1, large oscillations are experienced, as shown in figure 5. Even case 1, that is smoother exhibits higher oscillations than case 3.

Injection angle can consequently play an important role. Small angles tend to generate very thin, elongated vortices which are weak and are quickly damped. Large angles generate very thick vortices which may occupy space outside of the boundary layer and cause large oscillations without affecting advantageously the separation (not shown here).

It should be finally observed that the jet velocity amplitude levels of case 1 and 3 are higher than the external flow velocity, a fact which plays an important role in flow control.

Curiously, small changes in losses are observed with the addition of flow control, even when the deviation angle is decreased, that is separation is eliminated. This has been observed in the results obtained by other workers, and probably is related with the extensive mixing present during the active control procedure.

Finally, the discussions made above suggest that figures 1 and 4, help, orienting the designer towards the choice of the best solution, as well as in the formulation of a control strategy. They cannot provide the best solution per se. This can be done with the help of the URANS CFD simulation code, which may be used as an evaluator.

COMPRESSOR SURGE MARGIN GAIN

Computational simulation work has been performed concerning the surge margin gain, which is obtained by tip injection (for a

similar treatment see Leinhos et al. 2002, Nie et al 2002). It should be noted that although in the absolute frame of reference the tip injection is continuous, in the relative frame the rotor is sensing it as a pulsating inlet flow. This work has been realized in parallel with the experimental work performed on the rotor of the first stage compressor of the LARZAC engine in the Thermal Turbomachinery Lab of NTUA (see Kefalakis and Papailiou 2006). The available test rig power is not sufficient to drive the compressor at nominal conditions (18000 RPM, $\Pi=1.57$, $m_t=27.5\text{kg/sec}$), so part speed operation has been considered, that is an rpm range up to 11000 RPM, which corresponds to an approximately sonic relative inlet Mach number at the tip. Computations were performed for 9000RPM, $\Pi=1.16$ and $m_t=11.0\text{kg/sec}$, for which relative flow in the rotor is subsonic.

The solver used for the simulation has been developed in house. It uses an TVD-HLLC scheme, with variable extrapolation (MUSCL-like), 2^N tree adaptation, within a multiblock approach. It is parallelized using the MPI protocol. Additionally a variational structured grid generator is developed to complete the solver.

Tree adaptation is essential in order to accommodate computationally the installed jets. At the exit of each injection nozzle, the velocity is forced to assume the desired value of the injected velocity. The grid is locally adapted, in order to describe accurately the nozzle geometry (round hole or slot). This is illustrated in figure 6, where boundary cells of the casing are shown in the region of the nozzle proximity.

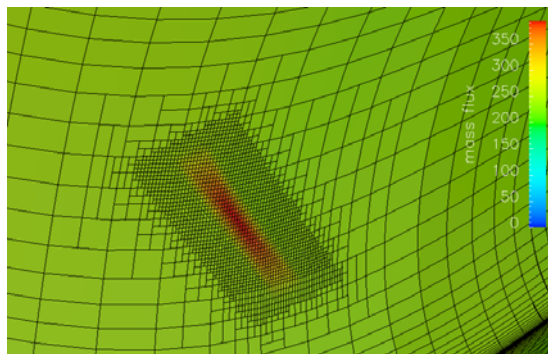


Figure 6: Grid adaptation at nozzle proximity

Using dynamic grid adaptation in the relative system of reference, the injection is simulated.

Before activating the flow injection, an initial steady state calculation is performed and used as the starting point for unsteady calculations. Certain assumptions have been accepted for the computational procedure, which are due, essentially, to the lack of availability of large computer capacity. The calculations were performed for one passage only, with cyclic periodicity conditions. Consequently, phenomena with different cyclic modes, such as rotating stall, could not be captured. On the other hand, in view of the short exit length available, appropriate acceleration, in order to avoid the presence of back

flow in the computational domain exit boundary, could not be imposed. In order to avoid computational break down, an artificial blockage was introduced by zeroing velocities at the exit boundary, when back flow was identified. The value of the blockage introduced to the flow was, in general, very small. Its magnitude will be given below along with the description of the calculation results. Finally, presently, the URANS solver does not possess the capability to compute laminar and transitional flow. This drawback, however, is not considered important for the present case, because, in view of the shape of the rotor blade velocity distributions, transition is taking place very early.

The number of injections installed peripherally was taken equal to the number of the rotor blades (23), rendering possible the simulation of only one passage. They were placed almost half a chord upstream of the leading edge on the casing, with a width of 0.9mm, a length of 16mm, and a skew of 45°, in agreement with the experimental configuration tested. The injection angle in respect to the casing (yaw) was equal to 15°. The mean injected relative velocity was 360m/sec (absolute velocity 160m/sec), that is 180% of the inlet relative velocity, resulting to a fraction of the compressor mass flow rate of 0.5%.

The first objective of the present work to be performed on the rotor, which is considered here, is to describe the flow conditions in the rotor passage during the onset of compressor stall. Steady state calculations used as a starting point indicate tip clearance vortex break down, observed as the operating point is approaching stall. This is illustrated in figures 7 (away from stall) where the tip clearance vortex is clearly present and 8 (very near stall), where the tip clearance vortex has broken down.

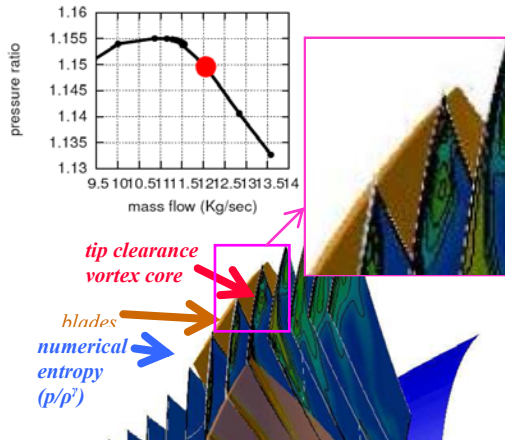


Figure 7: Steady state – seine operation

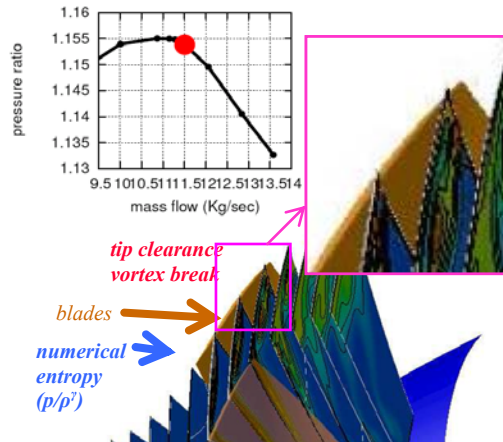


Figure 8: Steady state – tip clearance vortex breakdown

This indicates highly unsteady flow (see Furukawa et al 2000). Steady state calculations were performed for even lower mass flow rates, by throttling slowly the exit. The solver converged fast enough and followed the throttling. Only below of a mass flow rate of 9.5 kg/sec, artificial blockage became necessary.

A numerical experiment was performed, further, in order to verify whether tip injection could increase the stall margin of the compressor and simulate degradation of pressure rise and mass flow rate decrease, in stall conditions when control was turned off. A time accurate simulation was first set up with jets, at stall operating conditions for the no control case. Then, control was turned off, leading the compressor to stall. Calculation results are summarized in figures 9,10 and 11.

A computationally settling time of 6 blade passes is necessary, in order to obtain conditions of the compressor with jets turned on. The same settling time, almost equal to the time that a particle needs to travel up to the exit plane, is necessary in order to observe the start up of the drop of mass flow rate and pressure, characterizing compressor unstable operation, after jets are turned off.

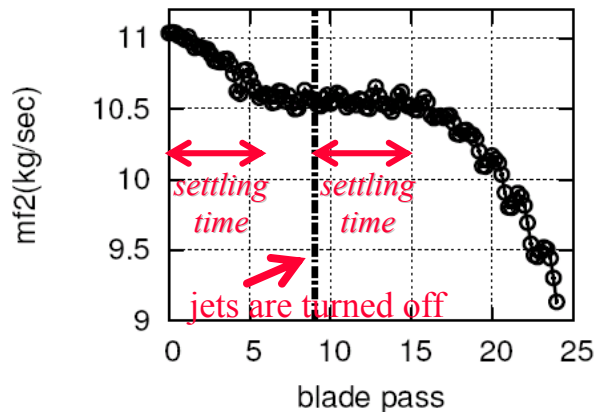


Figure 9: mass flow at exit plane

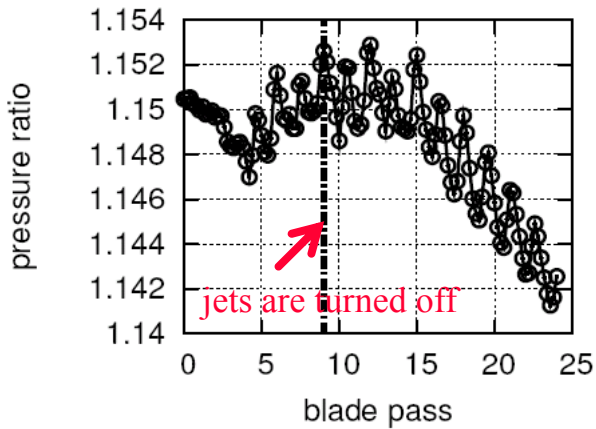


Figure 10: pressure ratio

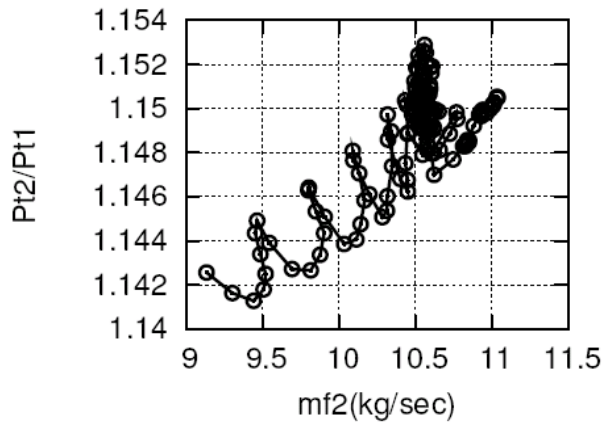


Figure 11: pressure ratio versus mass flow

This numerical experiment demonstrates that the mass flow considered initially (10.5kg.sec) is located in the compressor stall area for the uncontrolled case, but is found within the stable operation area, when control is applied. Consequently, once turning the jets off, the compressor can not maintain the static pressure set at the exit plane and the mass flow rate and pressure ratio deteriorate. It should be noted that during the simultaneous decrease of pressure ratio and mass flow rate, without control, the artificial blockage at the exit is practically zero and only, during the last two calculation points, it is increased to 14%.

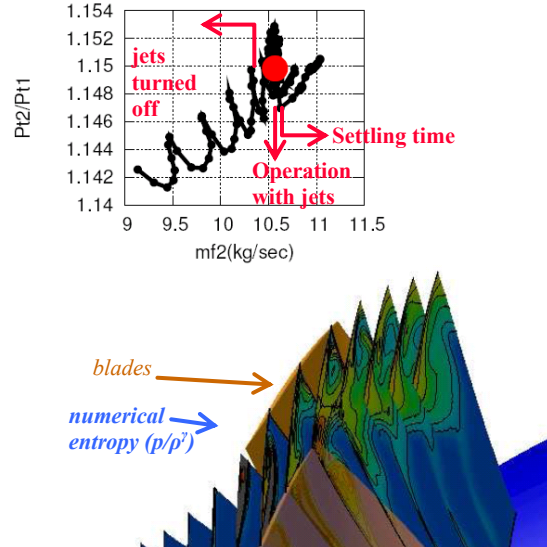


Figure 12: operation with jets

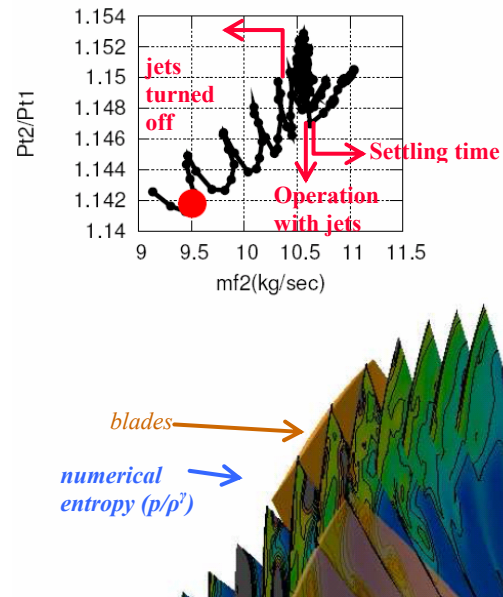


Figure 13: Operation without jets

The simulated flow field, with and without jets, was found to be highly unsteady. Strong vortical structures appear in the tip region, moving from the suction to the pressure side, resulting in oscillations of pressure ratio with a slightly different frequency than the one of blade passing frequency. As the jets pass in front of the passage, they tend to regulate these movements. This is why, as experimentally found (see Kefalakis and Papailiou 2006), the number of injection nozzles, which defines the forcing frequency of the flow, affects flow control. In figures 12 and 13 snapshots are given for with and without jets operating.

For the first case (figure 12), pressure ratio and mass flow rate are slightly oscillating, without any deterioration trends. However, the flow is highly unsteady and no tip clearance vortex structure is visible. For the second case (figure 13), the flow structure corresponding to the last operating point without control is shown, before artificial blockage at the downstream boundary of the calculation domain becomes appreciable. The flow field is again highly unsteady without trace of tip clearance vortex structure and the high loss area is quite increased, in comparison with the previous case.

CONCLUSIONS

In the present paper the first control case considered belongs to the internal aerodynamics domain (ducts, cascades). It is demonstrated that stability analysis, combined with a URANS solver are the two computational tools, which allow the optimization of the active flow control configuration necessary for reducing or eliminating existing separation regions. The developed computational tools allow to position the active flow control device and select the pulsation frequency and amplitude, in view of achieving an optimal configuration for flow control.

The second control case considered is that of a compressor rotor, for which optimal control is desired by use of tip flow injection. For this case a 3D URANS flow solver is developed and used for simulating continuous tip injection. Calculation results for a specific subsonic compressor rotor, are produced, which demonstrate the flow deterioration, when no control is used, inside the unstable operating region. Calculation results demonstrate also the URANS solver's capability to simulate controlled flow, which maintains operating conditions in the unstable area of operation without control. In both uncontrolled and controlled cases, highly flow unsteadiness and vortex brake down characterize the computed flow pattern, when approaching the compressor stall operating limit, without flow control.

REFERENCES

- Jeffrey P.Bons, Rolf Sondergaard and Richard B.Rivir. "Turbine separation control using pulsed vortex generator jets." In ASME Turbo Expo, number 2000-GT-0262, 2000
- Jeffrey P.Bons, Rolf Sondergaard and Richard B.Rivir. "The fluid dynamics of lpt blade separation control using pulsed jets." In ASME Turbo Expo, number 2001-GT-0190, 2001
- Masato Furukawa, Kazuhisa Saiki, Kazutoyo Yamada and Masahiro Inoue "Unsteady Flow behavior Due to Breakdown of Tip Leakage Vortex in an Axial Compressor Rotor at Near-Stall Condition." In ASME Turbo Expo, number 2000-GT-666, 2000
- David Greenblat and Israel J. Wygnanski. "The control of flow separations by periodic excitation". Progress in Aerospace Sciences, 36:487-545,2000
- M.Kefalakis and K.D.Papailiou. "Detailed Measurements on an Axial Compressorstage with application of discrete tip injection for increasing the surge marging", ETC,2006
- Dirk C.Leinhos, Scheidler Stephan G, and Leonhard Fottner. "Experiments in active control of a twin-spool turbofan engine." In ASME Turbo Expo, number 2002-GT-3002, 2002
- Chaoqun Nie, Gang Xu, Xiaobin Cheng and Jingyi Chen. "Micro air injection and its unsteady response in a low-speed axial compressor." In ASME Turbo Expo, number 2002-GT-30361, 2002
- H.Schlichting. "Boundary Layer Theory." Springer-Verlag, 8th edition, 2000, ISBN 3-540-66270-7
- Avi Seifert, La Tunia and G. Pack. "Oscillatory excitation of unsteady compressible flows over airfoils at flight Reynolds numbers." AIAA 99-925, 1999a
- Avi Seifert, La Tunia and G. Pack. "Active control of separated flows on generic configurations at high Reynolds numbers." AIAA 99-3403, 1999b
- Avi Seifert, La Tunia and G. Pack. "Sweep and compressibility effects on active separation control at high reynolds numbers." AIAA 2000-0410, 2000
- D. Skamnakis and K. Papailiou. "Flow stability analysis and excitation using pulsating jets". C.R. Mecanique, 333:628-635,2005
- D. Skamnakis and K. Papailiou. "Using Stability Analysis for Pulsating Jets Control Configuration". Submitted at FTC special issue for Flow Control, 2006
- W.Steiner, B.Eisenberg and H.Starken. "Design and testing of a controlled diffusion airfoil cascade for industrial axial flow compressor application." In ASME Turbo Expo, number 90-GT-140, 1990
- Ralph J.Volino. "Separation control on low pressure turbine airfoils using synthetic vortex generator jets." In ASME Turbo Expo, number GT2003-38729, 2003
- Zheng Xin-quian , Zhou Xia-bo and Zhou Sheng. "Investigation on a type of flow control to weaken unsteady separated flows by unsteady excitation in axial flows compressors". In ASME Turbo Expo, number GT2004-53167, 2004
- H.L.Zhang and H.F.Fasel. "Numerical investigation of the evolution and control of two-dimensional unsteady separated flow over a Stratford ramp." AIAA 99-1003, 1999

